Progress In Electromagnetics Research M, Vol. 90, 37–46, 2020

Low Sidelobe Wide Nulling Digital Beamforming for Large Planar Array Using Iterative FFT Techniques

Tarek Sallam[1, 2, *] and Ahmed M. Attiya[3]

Abstract—The combination of low peak sidelobe level (PSLL) with wide sector nulling digital beamforming (DBF) is achieved for large planar array antennas. This combination is carried out using the iterative Fourier transform (IFT) method. The method is based on the iterative Fourier technique to derive element excitations from the prescribed array factor using successive forward and backward Fourier transforms. A 1024-element rectangular uniformly spaced array is used as an example to demonstrate the performance of the proposed method. Numerical examples show that the proposed method achieves very low PSLL with very wide nulling sectors up to the half plane of the far-field pattern. Moreover, numerical results show that the proposed method is effectively functional even when the mainbeam is steered to directions other than the broadside.

1. INTRODUCTION

Modern communication, imaging, and sensing systems require using large antenna arrays to offer better capacity, higher resolution, and improved sensitivity. Examples of large array systems include massive MIMO systems [1], weather radar [2], satellite communication [3], and the next generation of radio telescopes [4]. Those systems increasingly rely on digital beamforming (DBF).

DBF is vital in advanced wireless systems. It is widely accepted that synthesis/optimization of beamforming could be tedious and time consuming procedure. Due to its complicated nature, most of these problems were solved by optimization algorithms like evolutionary algorithms with slow convergence and limited flexibility [5]. The nature of solving any DBF problem is to find a complex array weighting vector that leads to the desired radiation pattern.

The optimization approach considers nulling goals as a synthesis problem, where the weights are optimized to suppress sidelobes in the directions of interferers, i.e., enforcing the sidelobes to be smaller than a given threshold within a given sector. The optimization approach often allows one to satisfy other constraints, such as minimizing, at the same time the sidelobe level to fully exploit the degrees of freedom offered by the weights. Adaptive interference nulling [6], global optimizations [7–11], convex optimization [12], and multilayer antenna structures [13, 14] have been used to effectively suppress the sidelobes. The optimization approaches, however, are essentially iterative, which is time-consuming. On large arrays composed of hundreds to thousands of antenna elements, these optimization processes require huge computational time which rapidly becomes unaffordable.

A wide nulling problem is defined as producing a radiation pattern with a deep and wide spread sidelobe "nulling" at a certain direction while maintaining the mainlobe direction and other sidelobe level constants. Such a radiation pattern allows the DBF array to reject interference from certain direction without affecting the normal function. The problem is proven solvable by optimization algorithms [15],

Received 14 January 2020, Accepted 15 February 2020, Scheduled 2 March 2020

* Corresponding author: Tarek Sallam (tarek.sallam@feng.bu.edu.eg).

[1] Faculty of Electronic and Information Engineering, Huaiyin Institute of Technology, Huai'an, Jiangsu 223002, China. [2] Faculty of Engineering at Shoubra, Benha University, Cairo, Egypt. [3] Microwave Engineering Department, Electronics Research Institute (ERI), Giza, Egypt.

but when it is combined with getting low peak sidelobe level (PSLL), the problem becomes more and more complicated. Hence there is a demand for a fast, efficient, flexible, and practical solution to such problems, especially for large antenna arrays.

In [16], a genetic algorithm (GA) is proposed for the wide nulling of linear and circular arrays. By imposing an ideal template over the candidate patterns, multiple wide nulls of varying widths and depths are realized through altering the complex weights of the array elements. However, wider widths would come at a price of higher SLL, and besides GA's slowness prevents it from being used in real-time systems. In [17], an approach combining radial basis function neural network and GA (GA-RBFNN) is proposed for the wide nulling of linear array. The weights were computed using an RBFNN that approximates the GA solution. In this way, the slowness drawback of GA is solved, but at a price of a time consumed for training and testing the RBFNN. In [18], the bat algorithm (BA) and general regression neural network (GRNN) were applied to the wide nulling of linear arrays. The resulting data based wide nulling model shows the method of combining BA, and GRNN is more efficient and flexible than the traditional optimization algorithm based approach (i.e., using solely BA), but again at a price of additional burden of training and testing the GRNN.

This paper addresses a completely different approach for the low sidelobe wide nulling (LSWN) problem in DBF that is based on the iterative Fourier transform (IFT) method to synthesize patterns for array antennas with a periodic element arrangement [19]. The method uses the property that for an array having a uniform spacing of the elements, an inverse Fourier transform relationship exists between the array factor (AF) and the element excitations. Because of this relationship, a direct Fourier transform performed on the array factor will yield element excitations. The underlying approach relies on the repeated use of both types of Fourier transforms. At each iteration, the newly calculated array factor is adapted to the sidelobe requirements, and the result is then used to derive a new set of excitation coefficients. Only those excitation coefficients belonging to the array are used to calculate a new array factor. The key characteristics of this iterative synthesis method are simplicity and high robustness of its algorithm. The computational speed is very high, because the core calculations are based on direct and inverse fast Fourier transforms (FFTs).

It will be shown that the method can achieve low PSLL with wide sector nulling up to the half u-v plane of the far-field pattern for a 1024-element rectangular array. In addition, it will be demonstrated that the IFT method can deal with the LSWN problem even when the mainbeam is steered away from the broadside.

2. FORMULATION OF THE IFT METHOD FOR LSWN BEAMFORMING

The far field radiation pattern $F(u,v)$ of a rectangular planar phased antenna, with $M \times N$ elements arranged along a rectangular grid and spaced by d_x in the x-direction and d_y by in the y-direction, can be written as the product of element pattern F_e and array factor AF

$$F(u,v) = F_e(u,v)\, AF(u,v) \tag{1}$$

$$AF(u,v) = \sum_{m=0}^{M-1} \sum_{n=0}^{N-1} A_{mn} e^{jk(md_x u + nd_y v)} \tag{2}$$

where A_{mn} is the complex excitation of the (m,n)th element, k the free space wavenumber $(2\pi/\lambda)$, λ the wavelength, $u = \sin\theta\cos\phi$, and $v = \sin\theta\sin\phi$.

Equation (2) forms a finite double Fourier series that relates the element excitation coefficients A_{mn} of the array to its AF through a discrete inverse Fourier transform. AF is periodic in u-dimension over the interval λ/d_x and periodic in v-dimension over the interval λ/d_y. The rectangular region in u-v space covered by a single period of $AF(u,v)$ is given by

$$\left\{ -\frac{0.5\lambda}{d_x} \le u < \frac{0.5\lambda}{d_x} \text{ and } -\frac{0.5\lambda}{d_y} \le v < \frac{0.5\lambda}{d_y} \right\} \tag{3}$$

Through its double periodicity in u-v space, for any value of u and v, AF is equal to [20]

$$AF(u,v) = AF\left\{ \left[u - round\left(\frac{u}{\lambda/d_x} \right) \lambda/d_x \right], \left[v - round\left(\frac{v}{\lambda/d_y} \right) \lambda/d_y \right] \right\} \tag{4}$$

where the function *round* is defined as the nearest integer.

Since AF is related to the element excitations through a discrete inverse Fourier transform, a discrete direct Fourier transform applied on AF over the rectangle with dimensions λ/d_x and λ/d_y will yield element excitation coefficients A_{mn}. These Fourier transform relationships are used in an iterative way to synthesize LSWN patterns.

The iterative synthesis method consists of following simple seven steps:

1) Select an initial set of element excitations which is usually in uniform distribution;

2) Fourier transform the element excitations A_{mn} with a $K \times K$ points 2-D inverse FFT to arrive at the array factor AF consisting of $K \times K$ samples with $K >$ maximum $(M,\ N)$ by applying zero padding.

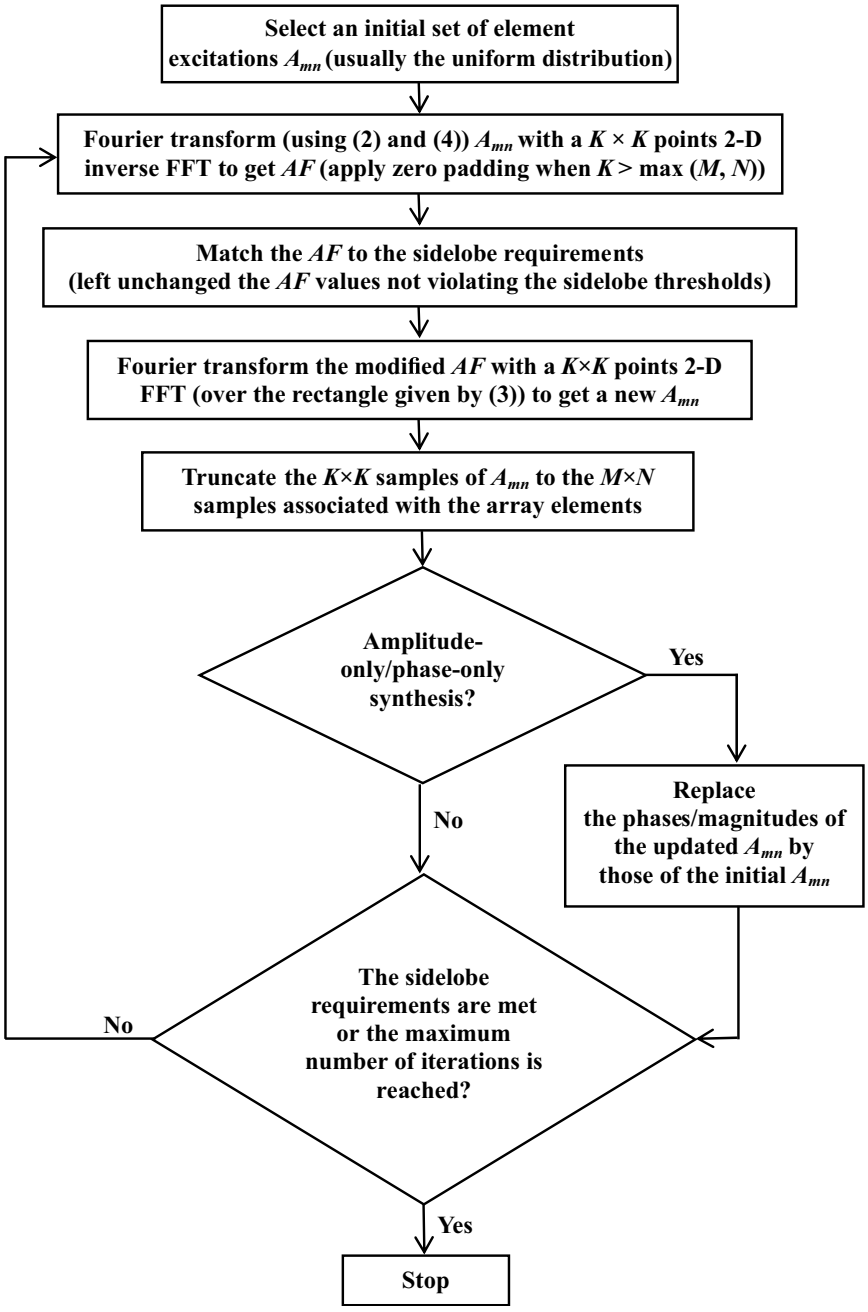

Figure 1. The flowchart of the IFT method.

3) Match the sidelobe region of AF to the sidelobe requirements and left AF values unchanged not violating the sidelobe thresholds like the AF values contained in the mainlobe region.

4) Fourier transform the modified AF with a $K \times K$ points 2-D FFT to get a new set of element excitations.

5) Truncate the $K \times K$ samples of element excitations to the $M \times N$ samples associated with the array elements.

6) Dealing with amplitude-only/phase-only synthesis replaces the phases/magnitudes of the updated element excitations by those of the initial element excitations of Step 1. By skipping Step 6, the LSWN pattern synthesis will be of the complex weighted type.

7) Repeat Steps 2 through 7 until the sidelobe region of AF of Step 2 matches the desired sidelobe characteristics or the maximum allowed number of iterations is reached.

The flowchart of IFT method is illustrated in Fig. 1.

Any low sidelobe AF consisting of $K \times K$ far field samples can be realized with $K \times K$ element excitations. This synthesis method arranges that the contribution of the excitations outside the aperture ($= K \times K - M \times N$ samples for a rectangular aperture) is transferred to the $M \times N$ excitations located inside the aperture.

The LSWN synthesis is performed in two successive resolution steps. During the second step, the same synthesis is performed as the first one, but with a higher number of points for the direct and indirect FFTs. The first resolution step is performed with 256×256 points while the second step applies 512×512 points direct and inverse FFTs. The output result of the first step, being the optimized element excitations, is used as input for the next step.

3. NUMERICAL RESULTS

A complex weighted LSWN synthesis at 10 GHz is applied to a rectangular array equipped with 1024 elements having an isotropic element pattern arranged in 16 rows and 64 columns with a square grid of inter-element pacing 0.015 m. The design objective is to obtain sidelobes of target PSLL at -45 dB with a nulling sector at -60 dB. All nulling sectors have $-1 \leq v \leq 1$.

With the mainbeam at broadside, the sector null starts from $u_{start} = 0.07$ to u_{end} which will be varied from 0.2 to 1 (i.e., the whole right half plane of the far-field pattern) with a step of 0.2. Fig. 2 shows a u-cut of the LSWN synthesized pattern through the mainbeam peak with u_{end} at 0.2. As can be seen, all far-field directions in the sidelobe region fit the prescribed sidelobe constraint of ≤ -45 dB. In the sector null, all sidelobes are below or at the goal PSLL of -60 dB except the first near-in sidelobe which is a little bit higher.

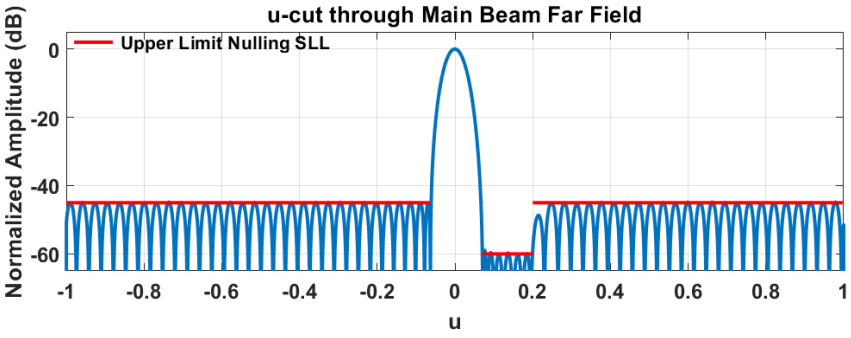

Figure 2. Far-field "u-cut" at $v = 0$ of the LSWN pattern when $u_{end} = 0.2$.

Figure 3 illustrates how the number of far-field directions exceeding the constraint of ≤ -45 dB for sidelobes and ≤ -60 for sector null decreases as the synthesis process progresses. The synthesis starts with a uniform distribution as the initial values that at the first iteration forms a pattern with 8808 far-field directions exceeding the sidelobe requirement in the sidelobe region and 2965 in the sector null. The whole synthesis involves 6698 iterations, of which 241 are spent during the first synthesis

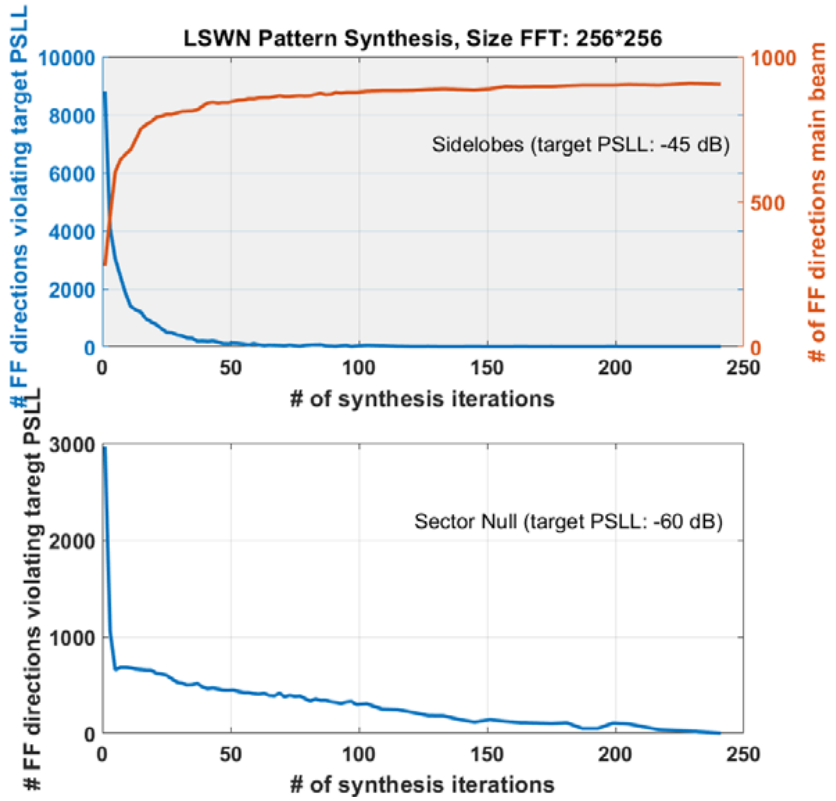

Figure 3. Number of far-field directions exceeding the target PSLL for sidelobes (in sidelobe region) and sector null along with the far-field inside the main beam during the first synthesis step of the pattern of Fig. 2.

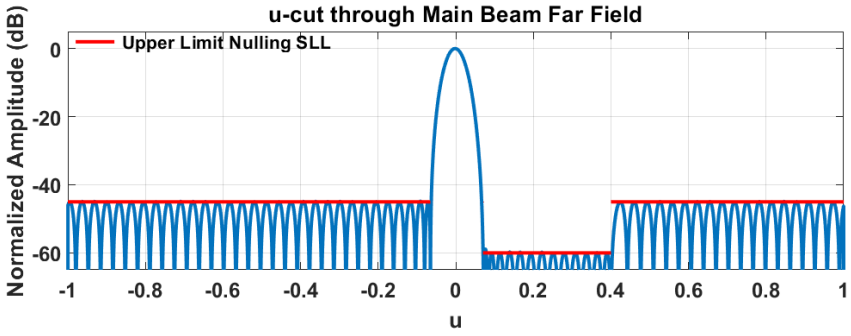

Figure 4. Far-field "u-cut" at $v = 0$ of the LSWN pattern when $u_{end} = 0.4$.

step carried out with 256×256 points FFTs and 6457 iterations for the second 512×512 resolution step. The total computational time to realize the result of Fig. 2 is less than 5 min (see Table 1). Fig. 3 shows also the widening of the mainbeam due to the decrease in sidelobe level. Moreover, Fig. 3 shows that although the sector null has fewer far-field directions exceeding the sidelobe requirement than the sidelobe region in the first iteration, most of the iterations are spent to fulfill the sidelobe requirement in the sector null.

Figures 4, 5, and 6 show the u-cut patterns when u_{end} equals 0.4, 0.6, and 0.8, respectively. Note that the sidelobe requirements are perfectly fulfilled in both the sidelobe region and sector null except only one or a few near-in sidelobes located immediately by the first mainbeam null on both sides of the mainbeam which exceed these requirements very slightly. On the other hand, Fig. 7 shows a 2-D pseudo

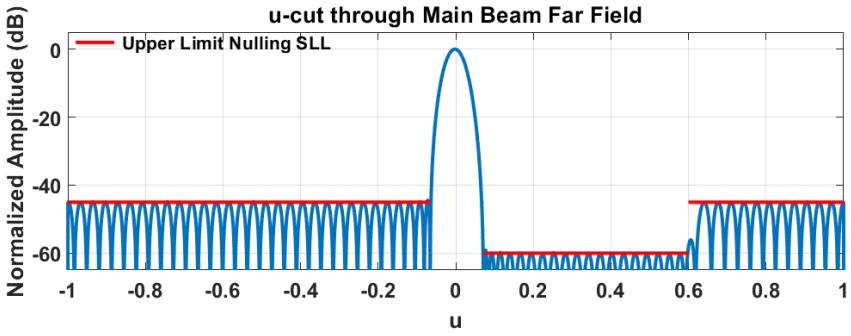

Figure 5. Far-field "u-cut" at $v = 0$ of the LSWN pattern when $u_{end} = 0.6$.

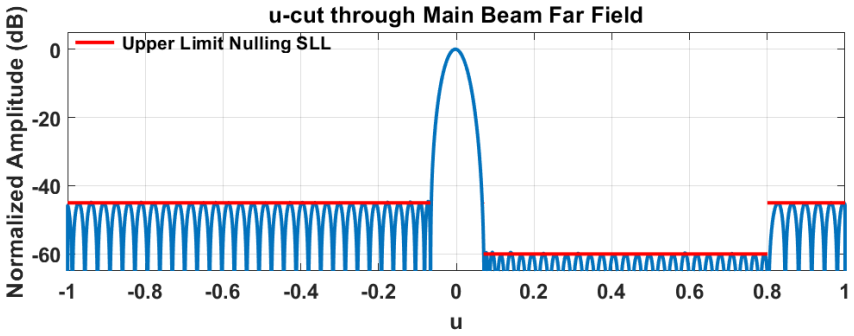

Figure 6. Far-field "u-cut" at $v = 0$ of the LSWN pattern when $u_{end} = 0.8$.

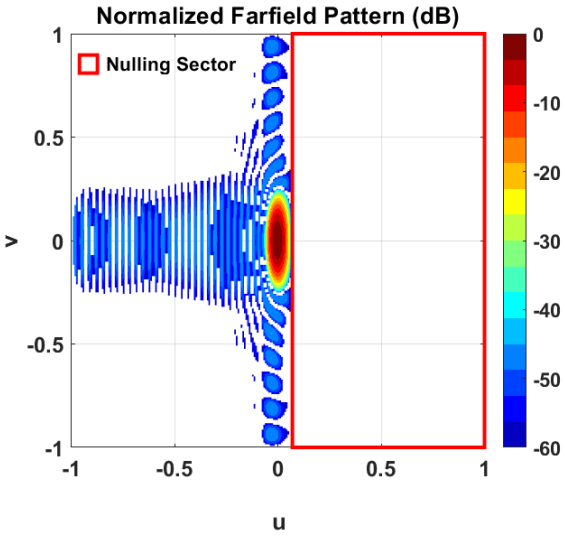

Figure 7. The 2-D pseudo contour plot of the LSWN far-field pattern when $u_{end} = 1$.

contour plot of the far-field pattern when $u_{end} = 1$. It can be noted that the whole right half plane of the far-field pattern is fully nulled (all directions with levels lower than -6 dB are zeroed (white area)). A u-cut of the far-field through the main beam peak is shown in Fig. 8. The associated amplitude distribution of the element excitations is depicted in Fig. 9(a). The corresponding phase taper is shown in Fig. 9(b). It can be noted that the amplitude distribution is smoothly curved. The sector nulling is completely the result of phase-only nulling and not of amplitude-only nulling due to the absence of diametrically located mirror nulled sectors, which are typical for amplitude-only sector nulling. In

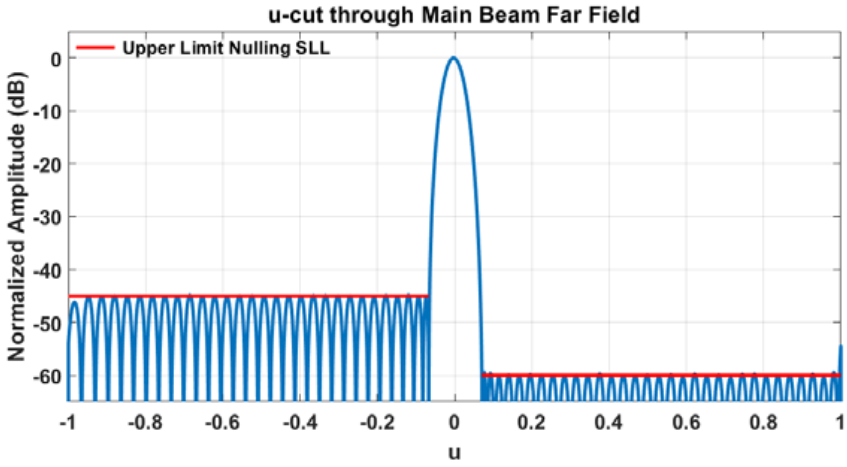

Figure 8. Far-field "u-cut" at $v = 0$ of the LSWN pattern of Fig. 7.

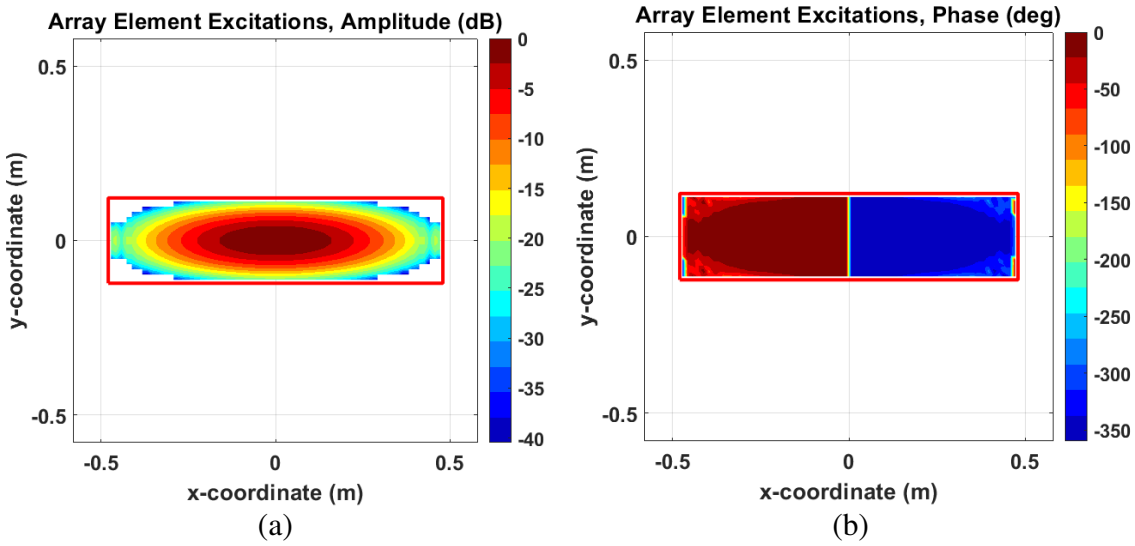

Figure 9. Aperture distribution pertaining to the pattern of Fig. 7. (a) Amplitude. (b) Phase.

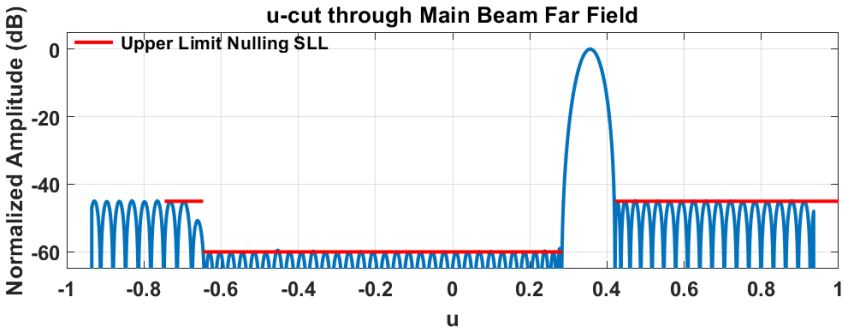

Figure 10. Far-field "u-cut" of the LSWN pattern steered to $(\theta, \phi) = (30°, 45°)$.

Fig. 9(b), the phase distribution in one half of the aperture is completely reversed in the other half which results in the suppression of a complete half plane of the far-field pattern as shown in Figs. 7 and 8.

Figure 10 demonstrates a wide nulling scenario when the mainbeam is steered to $\theta = 30°$ and $\phi = 45°$. The total nulling width is $u = 0.93$ which corresponds to about 57° nulling width. Also, for this steered beam, the PSLLs in both the sidelobe region and sector null obey the sidelobe requirements. The corresponding amplitude distribution is almost the same as in Fig. 9(a), while the phase taper responsible for this nulling is shown in Fig. 11. As can be seen, the phase distribution is linearly increasing (or decreasing) along the length of the rectangular aperture.

Table 1 presents the total CPU time along with the total number of iterations and the number of iterations spent during each resolution step to realize the LSWN patterns for each u_{end} as well as for the steering case. As can be noticed, in general, wider nulling sectors need more iterations as can be expected. Furthermore, except for relatively narrow nulling sectors (e.g., at $u_{end} = 0.2$), the majority of iterations are used during the first step.

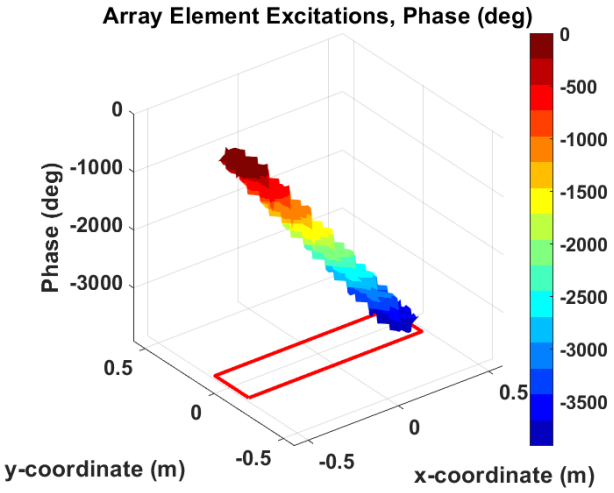

Figure 11. Aperture phase distribution pertaining to the pattern of Fig. 10.

Table 1. The total CPU time along with the total and each synthesis step number of iterations for each LSWN pattern.

LSWN pattern	Total CPU time (min)	Total # of iterations	# in 1st synthesis step	# in 2nd synthesis step
$u_{end} = 0.2$	4.70	6698	241	6457
$u_{end} = 0.4$	4.72	22562	18793	3769
$u_{end} = 0.6$	6.00	27194	21625	5569
$u_{end} = 0.8$	5.22	26138	23233	2905
$u_{end} = 1$	5.28	27386	24505	2881
Steered	4.61	26162	24601	1561

4. CONCLUSION

Different examples are presented in this paper to demonstrate that iterative FFT technique is quite suited for the synthesis of LSWN patterns for large planar arrays with periodic element spacing. The iterative Fourier technique can achieve low PSLL in addition to very wide nulling sectors up to a complete half plane of the far-field pattern. The presented results demonstrate that the proposed method is also quite effective to synthesize LSWN patterns in case the mainbeam is scanned away from broadside. It is found that all sidelobe directions of the achieved far-field match the prescribed sidelobe goals in both the

sidelobe region and sector null except the very close sidelobes on both sides of mainbeam. The iterative Fourier technique features a fast, robust, and quite simple method. The algorithm does not rely on parameters that have to be adjusted during their execution or a cost function that has to be minimized. Thus, it is very straightforward to be applied. Besides, the synthesis procedure does not make use of quadrant symmetry or any other symmetry property along the aperture. The computational time, as shown in Table 1, for the longest synthesis in this paper (this when u_{end} is 0.6) is 6 min on a PC with an Intel Core i7 processor running at 2.4 GHz and provided with 12 GB RAM.

REFERENCES

1. Larsson, E. G., O. Edfors, F. Tufvesson, and T. L. Marzetta, "Massive MIMO for next generation wireless systems," *IEEE Commun. Mag.*, Vol. 52, No. 2, 186–195, Feb. 2014.
2. Vollbracht, D., "System specification for dual polarized low power X-band weather radars using phased array technology," *Proc. Int. Radar Conf.*, 1–6, Lille, France, Oct. 2014.
3. Sallam, T. and A. M. Attiya, "Different array synthesis techniques for planar antenna array," *Applied Computational Electromagnetics Society Journal*, Vol. 34, No. 5, 716–723, 2019.
4. Bregman, J. D., "Concept design for a low-frequency array," *Proc. SPIE*, Vol. 4015, 19–33, Jul. 2000.
5. Xiao, X. and Y. L. Lu, "3D pattern optimization using PSO for an irregular dual-layer circular array," *Proc. 2018 IEEE International Symposium on Antennas and Propagation*, Boston, Massachusetts, Jul. 2018.
6. Ma, X., L. Lu, W. Sheng, Y. Han, and R. Zhang, "Adaptive interference nulling with pattern maintaining under mainlobe subspace and quadratic constraints," *IET Microw., Antennas Propag.*, Vol. 12, No. 1, 40–48, 2018.
7. Khodier, M. M. and C. G. Christodoulou, "Linear array geometry synthesis with minimum sidelobe level and null control using particle swarm optimization," *IEEE Transactions on Antennas and Propagation*, Vol. 53, No. 8, 2674–2679, Aug. 2005.
8. Van Luyen, T. and T. V. B. Giang, "Interference suppression of ULA antennas by phase-only control using bat algorithm," *IEEE Antennas Wireless Propag. Lett.*, Vol. 16, 3038–3042, 2017.
9. Oraizi, H. and M. Fallahpour, "Nonuniformly spaced linear array design for the specified beamwidth/sidelobe level or specified directivity/sidelobe level with mutual coupling consideration," *Progress In Electromagnetics Research M*, Vol. 4, 185–209, 2008.
10. Oraizi, H. and M. Fallahpour, "Sum, difference and shaped beam pattern synthesis by non-uniform spacing and phase control," *IEEE Transactions on Antennas and Propagation*, Vol. 59, No. 12, 4505–4511, Dec. 2011.
11. Oraizi, H. and M. Fallahpour, "Array pattern synthesis with mutual coupling consideration," *2008 International Symposium on Telecommunications*, 77–82, Tehran, 2008.
12. Fuchs, B., "Synthesis of sparse arrays with focused or shaped beam-pattern via sequential convex optimizations," *IEEE Transactions on Antennas and Propagation*, Vol. 60, No. 7, 3499–3503, Jul. 2012.
13. Nafea, S. N., A. Ismail, and R. S. A. Raja Abdullah, "Low side lobe level multilayer antenna for wireless applications," *Progress In Electromagnetics Research Letters*, Vol. 58, 105–111, 2016.
14. Nafea, S. N., "Improving performance of patch antenna for IEEE 802.16e applications using multilayer antenna structure with reflector," *2018 Al-Mansour International Conference on New Trends in Computing, Communication, and Information Technology (NTCCIT)*, 18–22, Baghdad, Iraq, 2018.
15. Van Luyen, T. and T. Vu Bang Giang, "BAT algorithm based beamformer for interference suppression by controlling the complex weight," *REV Journal on Electronics and Communications*, Mar. 2018.
16. Lu, Y. L. and B. K. Yeo, "Adaptive wide null steering for digital beamforming array with the complex coded genetic algorithm," *Proceedings 2000 IEEE International Conference on Phased Array Systems and Technology*, 557–560, Dana Point, CA, 2000.

17. Wang, Y. and Y. L. Lu, "The combination of neural networks and genetic algorithm for fast and flexible wide nulling in digital beamforming," *Proceedings of the 9th International Conference on Neural Information Processing*, 782–786, Singapore, 2002.
18. Xiao, X. and Y. L. Lu, "Data-based model for wide nulling problem in adaptive digital beamforming antenna array," *IEEE Antennas and Wireless Propagation Letters*, Vol. 18, No. 11, 2249–2253, Nov. 2019.
19. Keizer, W. P. M. N., "Planar phased-array antennas: Mutual coupling and ultra low peak sidelobes," *IEEE Antennas and Propagation Magazine*, Vol. 61, No. 1, 14–28, Feb. 2019.
20. Keizer, W. P. M. N., "APAS: An advanced phased-array simulator," *IEEE Antennas and Propagation Magazine*, Vol. 52, No. 2, 40–56, Apr. 2010.